Microfluid Nanofluid (2014) 16:455–464
DOI 10.1007/s10404-013-1238-1

RESEARCH PAPER

Numerical and experimental LDL transport through arterial wall

N. Filipovic · M. Zivic · M. Obradovic · T. Djukic · Z. Markovic · M. Rosic

Received: 20 February 2013 / Accepted: 18 July 2013 / Published online: 28 July 2013

Abstract Atherosclerosis develops from oxidized low-density lipoprotein molecules (LDL). When oxidized LDL evolves in plaque formations within an artery wall, a series of reactions occur to repair the damage to the artery wall caused by oxidized LDL. Aim of this study was to compare experimental data of LDL transport through isolated blood vessel with computational results of bounding of oxidized LDL receptor-1 (LOX-1) for endothelial cells with numerical discrete methods such as dissipative particle dynamics (DPD) and lattice Boltzmann (LB) method. Experiments of LDL transport were performed on the isolated rabbit common carotid arteries acquired from fifteen rabbits after 12 weeks of high-fat diet. Oxidative LDL molecule is built and used for docking with LOX-1 receptor. Energies that give the best binding are computed, and the energy with greatest probability of attachment for oxidative LDL molecule and glutamine acid is further used in numerical simulations. Simulations using DPD and LB method use the computed binding energy to calculate the force necessary for binding of LDL molecule to the endothelial blood vessel layer. Experimental results have shown large uptake for shear stress below 1 dyn/cm^2. Computational results for both discrete methods DPD and LB have shown good accuracy with experimental data. Calculation of the interactive molecule forces from computational chemistry open a new avenue for multiscale modeling methods, which will give better insight for the understanding and the prediction of LDL transport through the arterial wall for the medical community.

N. Filipovic (✉) · M. Obradovic · T. Djukic · M. Rosic
Faculty of Mechanical Engineering, University of Kragujevac, Kragujevac, Serbia
e-mail: fica@kg.ac.rs

N. Filipovic
Harvard School of Public Health, Harvard University, Boston, MA, USA

M. Zivic
Faculty of Biology, University of Belgrade, Belgrade, Serbia

Z. Markovic
State University Novi Pazar, Novi Pazar, Serbia

1 Introduction

Atherosclerosis is a chronic systemic inflammatory disease; the end-stage of which is plaque rupture. This depends on plaque composition and vulnerability rather than the severity of stenosis (Lusis 2000). Vulnerable plaques are associated with an intense inflammatory response and a thin fibrous cap (Hansson 2005). Remodeling and degradation of the extracellular matrix (ECM) and fibrous cap are maintained by the products of inflammatory cells (Libby 2002).

The LDL macromolecule enters through leaky junctions into the intima. There are two pathways of the LDL transport through the endothelium. Vesicles take up LDL from lumen by receptor-mediated endocytosis, whereas leaky junctions are associated with endothelial cells in a state of apoptosis (Lin et al. 1988).

The lectin-like oxidized low-density lipoprotein scavenger receptor (LOX-1) is an increasing focus of attention for molecular, cellular, and clinical studies. We investigate how the LOX-1 receptor and its ligand, oxidized low-density lipoprotein (oxLDL), are implicated at critical stages of plaque destabilization and rupture. Low-density lipoprotein(LDL) is made mainly by apolipoprotein B (apo B) and lipid molecules.

In order to pass endothelial barrier and enter arterial wall, oxLDL has to have the ability to bind to the endothelial cell membrane with sufficient strength to overcome shear forces for a sufficient period of time so that the transport could be accomplished. The binding site on the luminal part of endothelial cell membrane must have appropriate characteristics. LOX-1 has emerged as the prime candidate, because it fulfills the requirements. Namely, LOX-1 is a member of heterogeneous group of scavenger receptors that is able to bind, internalize, and degrade oxLDL, but not native LDL (Reiss et al. 2009). Also, LOX-1 is the only member of the mentioned group of receptors that is significantly expressed in endothelial cells (Bickel and Freeman 1992; Sawamura et al. 1997), making it the major receptor facilitating the binding and uptake of oxLDL by endothelial cells. Therefore, it is a molecule of interest in this study. In addition, several facts demonstrate the important role of LOX-1 in different stages of atherogenesis from the very onset until the end: (1) Ox-LDL activates LOX-1 and induces endothelial dysfunction/apoptosis (Li and Mehta 2000a, b), which is a major change in vascular biology seen at the beginning of atherogenesis; (2) besides ox-LDL, there are other mediators of atherosclerosis that upregulate LOX-1, such as angiotensin II (Ang II) cytokines, shear stress, advanced glycation end products (AGE); (3) LOX-1 is dynamically upregulated by pro-atherogenic conditions, such as diabetes, hypertension, and dyslipidemia (Chen et al. 2000; Nagase et al. 1997; Kume et al. 1998; Murase et al. 1998); and (4) LOX-1 is present in atheroma-derived cells and is observed in large amounts in human and animal atherosclerotic lesions in vivo (Chen et al. 2000; Kataoka and Miyamoto 1999).

Apo B is part of the LDL, which contains 4,536 amino acid residues distributed in eight domains. Domain 4 and domain 5 are very important because they ensure further interaction with receptor on the binding sites (Kriško and Etchebest 2006). The receptor of interest in this study LOX-1 is also made of the chains of amino acid residues, but it contains a lower number of amino acids in its structure than an apo B structure. LOX-1 contains only 256 amino acid residues. LOX-1 is the receptor that is bound with the protein part of LDL molecule, apo B.

LDL contains in its structure molecules which are easily oxidized. LDL interacts with the receptor under its oxidized LDL form. In the fifth domain, where we studied the interaction, there are 27 lysines. Lysine residues are easily carbamylated by cyanate. So, for oxidative modification of LDL, HOCN molecule is used. Carboxylic group of lysine is reacted with cyanate anion, which makes formation of modified lysine. Oxidative LDL molecule is built and used for docking with LOX-1 receptor.

Among several LDL transport models, three major categories exist. The simplest models are wall-free models, in which the arterial wall is substituted by a simplified boundary condition. Rappitsch and Perktold (1996) and Wada and Karino (2000) applied these models for the analysis of the macromolecular transport in the arterial wall. A more realistic approach is used in lumen-wall models, where there is a coupling of the transport within the lumen and the wall (Moore and Ethier 1997; Stangeby and Ethier 2002a, b). Also there are multilayer models, which break the arterial wall down into several layers and model the transport within the wall, either at the microscopic (Yuan et al. 1991; Huang et al. 1994; Huang and Tarbell 1997; Tada and Tarbell 2004) or at the macroscopic (Fry 1985, 1987; Karner et al. 2001) levels. However, there are few numerical studies that rely on real experimental data for LDL transport.

The DPD method is a discrete modeling technique, which consists of particles that correspond to coarse-grained entities as molecular clusters and not to individual atoms (Hoogerburgge and Koelman 1992). It is a very effective technique in simulating mesoscopic hydrodynamics of simple and complex liquids (Espanol and Warren 1995; Groot and Warren 1997).

Lattice Boltzmann method belongs to the class of methods named Cellular Automata (CA). This means that the physical system can be observed in an idealized way, so that space and time are discretized, and the whole domain is made up of a large number of identical cells (Wolfram 1986). A number of particles that move and collide in discrete time–space domain are observed, and dynamics of these particles are modeled. In LB model, in every lattice node (representing one particle), it is necessary to define one real number—the particle distribution function.

In this study, we first describe the experimental setup for the LDL transport into the blood vessel wall in the isolated rabbit carotid artery under physiologically relevant constant pressure and perfusion flow on rabbits with 12-week high-fat diet. Then, we show the computational procedure for calculation of energies that give the best binding and that have the greatest probability of attachment of oxidative LDL molecule with endothelial cells. DPD and LB methodologies are then shortly described. Comparison of the numerical results with DPD and LB methods is given, as well as some discussion and conclusions are provided.

2 Materials and methods

2.1 Experimental setup

Ex vivo blood vessels experiments of LDL transport were performed on the isolated rabbit common carotid arteries. Experiments were performed according to the Animals Scientific procedures Act 1986 (UK) and local ethical

guidelines. New Zealand White rabbits of both sex weighing 3.5–4 kg were anesthetized using Ketamine (Laboratorio Sanderson, Santiago, Chile), 4–6 mg per kg of body weight. Blood vessel was excised and placed in the water bath. Cannulas with equally matched tip diameters (2 mm) were mounted at proximal (cardial) and distal (cranial) ends of the blood vessel. The lumen was perfused with Krebs–Ringer physiological solution (KRS), using the peristaltic pump at 1 ml/min. The perfusate was continuously bubbled with a 95 % O_2 and 5 % CO_2 with the pH adjusted to 7.4 at 37 °C.

The distal cannula was connected to the resistance changing device. Perfusion pressure was measured with perfusion transducer (Fig. 1).

The blood vessel was stretched to its approximate in vivo length. The outer diameter of the blood vessel was measured using digital camera and originally developed software. The blood vessel wall thickness was measured at the end of each experiment, using light microscope and microscopically graduated plate (see Fig. 2).

The isolated blood vessel was placed into the water bath with physiological buffer. After the equilibration period (20–30 min) at constant perfusion flow of 1 ml/min, 100 µl bolus was injected into the perfusion system containing ^{99m}Tc-Nanocis as an intravascular marker (referent tracer), or ^{125}I-LDL as a test molecule. The first 15 samples (3 drops in each sample) and 9 cumulative 3-min samples of perfusion effluent were sequentially collected. All samples were prepared for measurement of ^{125}I-LDL-specific activity by addition of physiological buffer until final volume of 3 ml/sample. Measurements of perfusion effluent samples containing ^{99m}Tc-Nanocis or ^{125}I-LDL were taken by means of the gamma counter (Wallac Wizard 1400, GMI, Inc. Minnesota, USA).

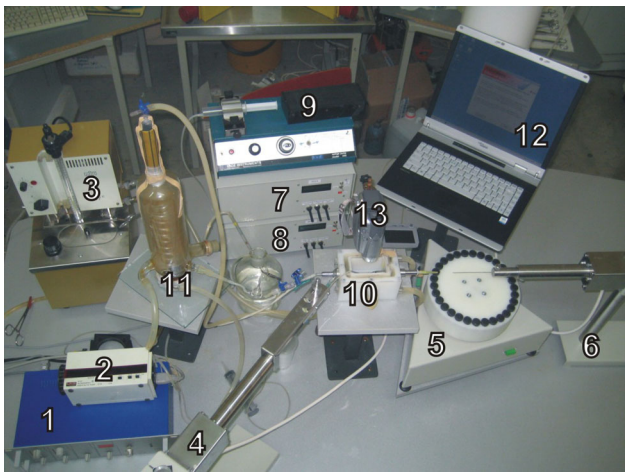

Fig. 1 Setting for ex vivo blood vessels experiments: *1* Pressure and temperature A/D converter, *2* Peristaltic pump, *3* Heater thermostat, *4* Rapid infusion pump (RIP), *5* Automatic sampler, *6* Resistance changing device (RCD), *7* Control unit for RIP, *8* Control unit for RCD, *9* Syringe infusion pump, *10* Water bath, *11* Heating stabilizer, *12* PC, *13* Digital camera

The ^{125}I-LDL uptake is derived from the difference between the ^{99m}Tc-Nanocis value and that of ^{125}I-LDL recovery in each sample.

2.2 Chemical computational methods

The structures of LOX-1 and apo B (all eight fragments) were provided from the Protein Data Bank (1YXK.pdb, Ohki et al. 2005), domain 5-1VPK_A.

For the purpose of this investigation, Lys from domain 5 of apoB was modified according to Fig. 3. The modified domain 5 of apoB was used for docking of LOX-1.

2.2.1 Docking

A protein properties calculator has recently been developed in the Molecular Operating Environment (MOE) (Chemical Computing Group Inc. Montreal). This tool allows to process one or more proteins and compute a series of protein-specific descriptors. MOE-Dock uses Amber force field to calculate interaction energies between the ligand and the receptor.

The modified Lys from domain 5 of apoB (ligand) was docked into LOX as a receptor. A docking box of 125 × 125 × 125 grid points with 0.375 Å spacing between each grid point was used. The docking box was centered on the docked conformation of the modified Lys. The threshold was chosen based on the values of the docking energies. On the basis of the obtained values of docking energies, structures with the smallest energies were selected. In the next step, only the structures where the modified Lys is proximate to the amino acids of LOX-1 (30 nm or less) were used for further investigations.

2.2.2 Mopac

PM6 Hamiltonian (Stewart 2007) from MOPAC 2009™ program package (available online, MOPAC 2009) was used to optimize reaction paths between modified Lys and aspartic and glutamic acids, and cysteine. The criterion for terminating all optimizations was increased 100-fold over normal MOPAC limits using the PRECISE option. All structures were characterized as stationary points or transition states on the potential energy surfaces, using the keyword FORCE. The criterion for a minimum is when all eigenvalues of the Hessian matrix are positive, while for the transition state, only one eigenvalue is negative. The IRC calculations were performed to confirm that each saddle point is a transition state indeed.

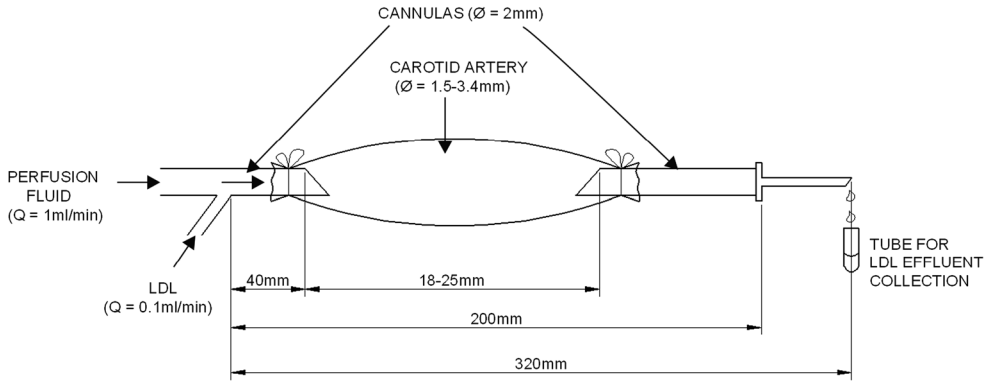

Fig. 2 Schematic presentation of the isolated blood vessel segment in the water bath

Fig. 3 Modification of Lys from domain 5 of apoB with HOCN

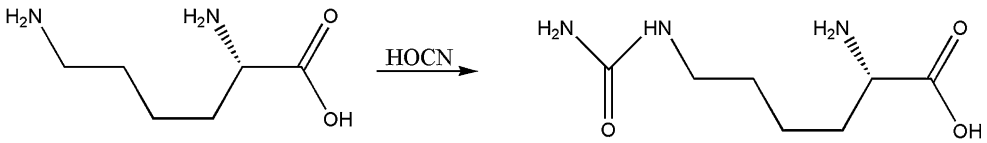

To estimate bond energy between the modified Lys and amino acids of LOX-1, energy partitioning of the one- and two-center terms was performed for all reactants, transition states, and products, using the keywords ENPART and 1SCF.

On the basis of the defined criteria, the docking analysis showed that the modified Lys of apoB mainly reacts with aspartic acid (Asp), glutamic acid (Glu), and cysteine acid (Cys) of the LOX-1. To determine the intensity of these interactions, corresponding reaction paths were simulated with PM6 method. All three transition states were found. The energy barriers for the reactions between modified Lys and Asp, Glu, and Cys amount to 88.89, 126.87, and 165.78 kJ/mol, respectively. Based on the activation energies, it is clear that the reaction with aspartic acid is the fastest. Using the ENPART option from MOPAC 2009^{TM} (available online, MOPAC 2009), the bond energies of the newly formed C–N bond, along the reaction pathway, were calculated. The results are given in Table 1.

Table 1 Bond energies for C–N bond between modified Lys and amino acids of LOX-1

C–N bond	Bond energies of C–N bond (J)		
Bond length (m)	Glu–Lys	Asp–Lys	Cys–Lys
1.46E−10	−2.65E−18	−2.44E−18	−2.48E−18
1.56E−10	−2.38E−18	−2.20E−18	−2.23E−18
1.66E−10	−2.12E−18	−1.95E−18	−1.98E−18
1.76E−10	−1.88E−18	−1.72E−18	−1.73E−18
1.86E−10	−1.67E−18	−1.47E−18	−1.50E−18
1.96E−10	−1.48E−18	−9.66E−19	−1.28E−18
2.06E−10	−7.82E−19	−8.01E−19	−1.09E−18
2.16E−10	−6.50E−19	−6.79E−19	−9.25E−19
2.26E−10	−5.47E−19	−5.88E−19	−7.89E−19
2.36E−10	−4.67E−19	−5.21E−19	−6.80E−19
2.46E−10	−4.08E−19	−4.71E−19	−3.74E−19
2.56E−10	−3.66E−19	−4.33E−19	−3.40E−19
2.66E−10	−3.35E−19	−4.00E−19	−3.15E−19
2.76E−10	−3.11E−19	−3.73E−19	−2.95E−19
2.86E−10	−2.93E−19	−3.51E−19	−2.78E−19
2.96E−10	−2.78E−19	−3.36E−19	−2.57E−19
3.06E−10	−2.65E−19	−3.19E−19	−2.47E−19

2.3 Computational methods for DPD

Dissipative particle dynamics is a mesoscopic simulation technique. Basic principle of the method is the fact that all particles interact with the neighboring particles, which are in a certain domain and force of interaction consists of three inner forces: conservative, dissipative (because of stochastic behavior), and random force.

$$f_i = \sum_{j \neq i} \left(F_{ij}^C + F_{ij}^D + F_{ij}^R \right) \quad (1)$$

Movement of each DPD particle is directed by the second Newtonian law:

$$m_i \dot{v}_i = \sum_j \left(F_{ij}^C + F_{ij}^D + F_{ij}^R \right) + F_{ij}^{ext} \quad (2)$$

where m_i is the mass of particle, $\dot{v}_i$ is acceleration, $F_{ij}^C, F_{ij}^D, F_{ij}^R$ are, respectively, conservative, dissipative, and random force, and F_{ij}^{ext} represents external force, usually gradient of pressure or gravitational force.

For the binding of LDL molecules on the arterial wall, the spring force is used (Filipovic et al. 2008a, b):

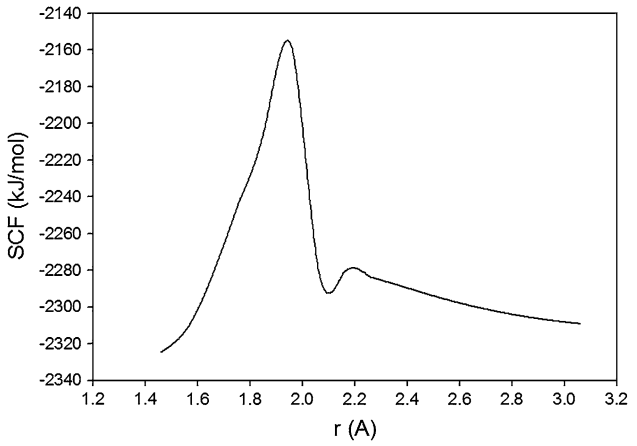

Fig. 4 Dependence between energies and distances of molecules of LDL and glutamine acid

$$F_a = k_{sf}(1 - \frac{L_{sf}}{L_{sf}^{\max}}) \tag{3}$$

where L_{sf} is the distance between the molecule of LDL and the endothelium, $L_{sf}^{\max}$ is the maximum distance between molecules, and k_{sf} is the stiffness coefficient.

The spring force coefficient was obtained from chemical measurements of binding energy between LDL molecule and receptor from endothelium. As it was concluded in Sect. 2.2, molecule of LDL needs three receptors for binding, so the force coefficient was calculated as a triple value of one chemical component.

Computed energies that give the best binding with greatest probability of attachment are plotted in Fig. 4. This diagram represents dependence between energies and distances of molecules of LDL and glutamine acid.

As it can be seen from Fig. 4 at distance 1.86 A (1 A = 10^{-10}m), the transition state occurs, where the connection between LDL molecule and the receptor can be broken. For stable binding, distances need to be in the range of 1.46–1.86 A while binding breaks at greater distances.

We calculated the force between molecules as ratio of obtained energies to measured distances. For calculation of the spring stiffness coefficient in Eq. (3), we used diagram from Fig. 4. For example, at distance 1.76 A and obtained energy 1.88256×10^{-18} J, the calculated force is 1.07×10^{-8} J/m. The stiffness coefficient is 60.775 kg/s. That value is tripled because we modeled one spring for binding of LDL molecule and three receptors on the endothelium.

2.4 LB methods

Lattice Boltzmann method belongs to the class of methods named Cellular Automata (CA). This means that the physical system can be observed in an idealized way, so that space and time are discretized, and the whole domain is made up of a large number of identical cells (Wolfram 1986). A number of particles that move and collide in discrete time–space domain are observed, and dynamics of these particles are modeled. In LB model, in every lattice node (representing one particle), it is necessary to define one real number—the particle distribution function. Special propagation function is defined that depends on the state of neighboring cells and it has an identical form for all cells. The state of all cells is updated synchronously, through a series of iterations, in discrete time steps. The advantages of this method are the simple implementation, the stability of the solution, easy assignment of boundary conditions, and natural parallelization.

The basic equation of LB method is the Boltzmann equation. The equations that are used to simulate fluid flow are derived from the Boltzmann equation. Afterward, these equations are discretized in order to be numerically solved. The Boltzmann equation is a partial differential equation that describes the behavior and movement of particles in space, based on a single distribution function f. This distribution function is defined in such a way that $f(\mathbf{x}, \mathbf{v}, t)$ represents the probability for a particle to be located within a specific space element ($\mathbf{x}$, $\mathbf{v}$) at time t, where $\mathbf{x}$ and $\mathbf{v}$ are the spatial position vector and the particle velocity vector, respectively.

In the presence of an external force field $\mathbf{g}$, it is possible to write a distribution function balance equation—Boltzmann equation:

$$\frac{\partial f}{\partial t} + \mathbf{v}\frac{\partial f}{\partial \mathbf{x}} + \frac{\mathbf{g}}{m} \cdot \frac{\partial f}{\partial \mathbf{v}} = \Omega \tag{4}$$

where m is the mass of a particle, and Ω is the collision operator that represents the changes in the distribution function due to the inter-particle collisions.

Since this operator is represented using a very complex expression, a simplified model is introduced, initially proposed by Bhatnagar et al. (1954). An assumption is made that the effect of collision between particles is to drive the fluid toward a local equilibrium state. This model is known as the single relaxation time approximation or the Bhatnagar–Gross–Krook (BGK) model. Operator Ω is defined as follows:

$$\Omega = -\frac{1}{\tau}\left(f - f^{(0)}\right) \tag{5}$$

where τ is the relaxation time (the average time period between two collisions), and $f^{(0)}$ is the equilibrium distribution function—so-called Maxwell–Boltzmann distribution function.

The original BGK Boltzmann equation is valid for continuum and is not suitable for numerical

implementation. The discretization procedure has to be performed in such a manner that the Navier–Stokes equations can still be derived from the newly obtained equations and this procedure is described in the literature (Malaspinas 2009; Đukić 2012). The final form of the LB equation that is numerically solved is given by:

$$f_i(\mathbf{x}+\mathbf{v}_i,t+1)-f_i(\mathbf{x},t)=-\frac{1}{\bar{\tau}}(f_i(\mathbf{x},t)-f_i^{eq}(\mathbf{x},t))+\left(1-\frac{1}{2\bar{\tau}}\right)\mathbf{F}_i \quad (6)$$

where $\bar{\tau}$ is the modified relaxation time that was introduced to provide better numerical stability of the solution and to enable explicit time steps and thus a more appropriate time discretization. In numerical simulations, the whole calculation process is conducted using the modified relaxation time. In the Eq. (6), $\mathbf{F}_i$ represents the discretized force term.

The macroscopic quantities of fluid flow are evaluated in terms of the distribution function. Fluid density and velocity can be calculated as weighted sums over a finite number of discrete abscissae that were used to discretize the space domain:

$$\rho=\sum_i f_i \quad (7)$$

$$\bar{\mathbf{u}}=\frac{1}{\rho}\sum_i \mathbf{v}_i f_i=\frac{1}{\rho}(\rho\mathbf{u}-\rho\mathbf{g}/2) \quad (8)$$

where $\mathbf{v}_i$ is the vector defining the direction of ith abscissa.

When LB method is implemented on a computer, Eq. (6) is solved in two steps: (1) collision and (2) propagation. Two values of the distribution function can be defined—f_i^{in} and f_i^{out}, that represent the values of the discretized distribution function before and after the collision, respectively. The mentioned steps are expressed as follows:

Collision step:

$$f_i^{\text{out}}(\mathbf{x},t)=f_i^{\text{in}}(\mathbf{x},t)-\frac{1}{\bar{\tau}}\left(f_i^{\text{in}}(\mathbf{x},t)-f_i^{(0)}(\rho,\mathbf{u})\right)+\left(1-\frac{1}{2\bar{\tau}}\right)\mathbf{F}_i \quad (9)$$

Propagation step:

$$f_i^{\text{in}}(\mathbf{x}+\mathbf{v}_i,t+1)=f_i^{\text{out}}(\mathbf{x},t) \quad (10)$$

Each one of these steps must be applied to the whole system (to all particles) before the next one starts. The step that considers collisions is a completely local operation, and therefore, the equilibrium distribution function is calculated in every lattice cell individually, in every time step, in terms of density ρ and macroscopic velocity $\mathbf{u}$. The step that considers propagation communicates with only a few neighbors.

2.4.1 Modeling particle–fluid interaction

In this study, we also focused on modeling the movement of LDL particles in blood flow using LB method. That practically means that particles (LDL molecules) and fluid (blood) are forming a coupled mechanical system. We used the particle tracking method, and results obtained with this method are compared with experimental results.

In this approach, the fluid flow is completely solved (until steady state is reached). The LDL particles are fixed inside fluid domain during this part of the simulation. At the end of the fluid flow simulation, the movement of LDL particles is analyzed. It is possible to determine the force and momentum acting on the LDL particle, which are exerted from the fluid flow. It is considered that the velocity of fluid and LDL particle in $\times$ direction is equal, and therefore, for X axis, the following equation is valid:

$$\frac{\mathrm{d}x_p}{\mathrm{d}t}=v_{px}=u_{fx} \quad (11)$$

where indexes p and f denote particle and fluid related quantities, respectively.

In y direction, the effect of fluid on LDL particle can be neglected, because the fluid flow is assumed to be shear flow (the y velocity component is equal to zero). The equation of particle motion along y direction is therefore given by:

$$m\frac{\mathrm{d}}{\mathrm{d}t}\left(\frac{\mathrm{d}y_p}{\mathrm{d}t}\right)=F_{py} \quad (12)$$

where m is the LDL particle mass (which is assumed to be equal to 1), and F_{py} is the force acting on LDL particle that is attracting it toward the bottom wall. This force is calculated based on the computational chemistry simulations that are explained in Sect. 2.2. The same formula that is used for DPD simulations is used in LB simulations as well and is given in Eq. (3). This effect is implemented in such a way that once the LDL particle is close enough to the wall, a chemical reaction force is acting on this particle, preventing any further movement of the particle.

It is assumed that the LDL particle is very small, and thus, its rotation can be neglected because it has no importance for the overall particle motion. Integrating Eqs. (11) and (12), the coordinates of the LDL particle are obtained. These two equations are integrated with new data in an iteration loop, until the LDL particle collides with one of the boundaries of the domain. The schematic diagram of the described procedure is shown in Fig. 5.

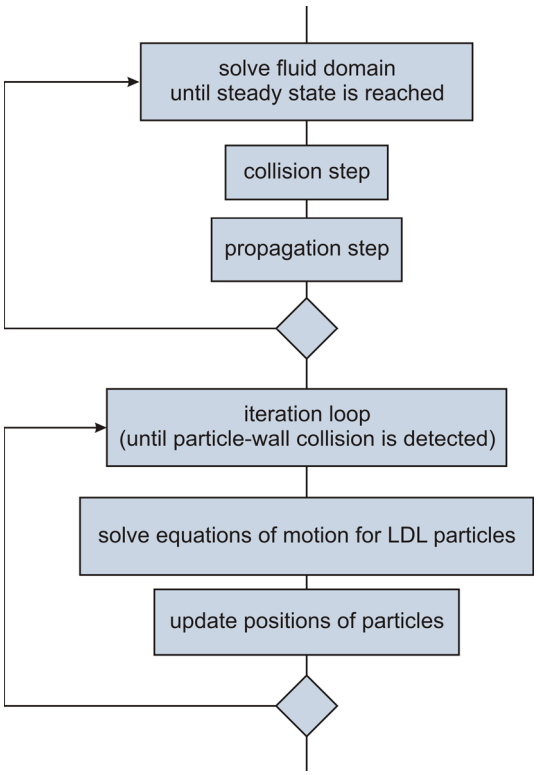

Fig. 5 Algorithm of the particle tracking approach

3 Results

Experimental results for shear stress effects on the steady-state LDL uptake are shown in Fig. 6. It can be observed that for low shear stress, below 1 dyn/cm^2, there is a large LDL uptake on the isolated blood vessel. After fitting experimental data, an exponential curve can be obtained:

$$u_p = 0.898 \cdot \sigma^{-0.5507} \tag{13}$$

where σ denotes the shear stress and u_p is the uptake percentage.

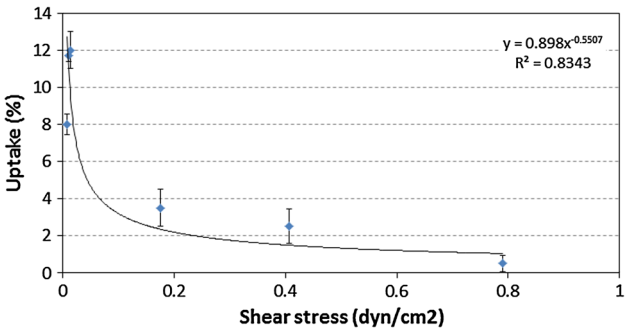

Fig. 6 Experimental results for shear stress effects on the steady-state LDL uptake

for seven different values of shear stress. Values of applied shear stresses and appropriate shear rates are connected with the following equation:

$$\sigma = \mu \cdot R \tag{14}$$

where μ is the dynamic viscosity and R is the shear rate. In this case, the dynamic viscosity is equal to 0.035 Pa · s.

The number of particles in DPD simulations along the x and y axis is 2,500 and 360, respectively. These dimensions of the computational domain are determined according to the experimental setup. Time step is 0.0015 s, and number of time steps is 10^7, so the total time of calculation is 14.167 h.

For the binding of LDL molecules on the blood wall, a spring force was used. Coefficient of spring force was obtained from chemical measurements of binding energy between LDL molecule and receptor from endothelium. One LDL molecule needs three receptors for binding, so our coefficient was calculated as triple value of one chemical component.

For different values of applied shear stress, shear rate was calculated based on the predefined dynamic viscosity of blood and dimension of the model.

Total number of LDL molecules in the model is 111, or 0.13 ‰ of the total number of fluid particles.

We calculated the number of bound LDL molecules 15 times for all considered values of shear stress. Different numbers of bound LDL molecules for the same shear stress originate from random position of LDL molecules in the start of calculation.

The third calculation	15.31532	13.51351	6.306306	3.603604	1.801802	1.801802	0

3.1 DPD results

First, we used DPD methodology to simulate binding of LDL molecules on the endothelium layer for different values of applied shear stress, and then, we compared the obtained results with experimental results. Number of bound LDL molecules or percent of binding was calculated

DPD simulation results and their comparison with experimental results are shown in Fig. 7.

3.2 LB results

The simulation is performed in a rectangular domain, and geometrical data are shown in Fig. 8. The boundary

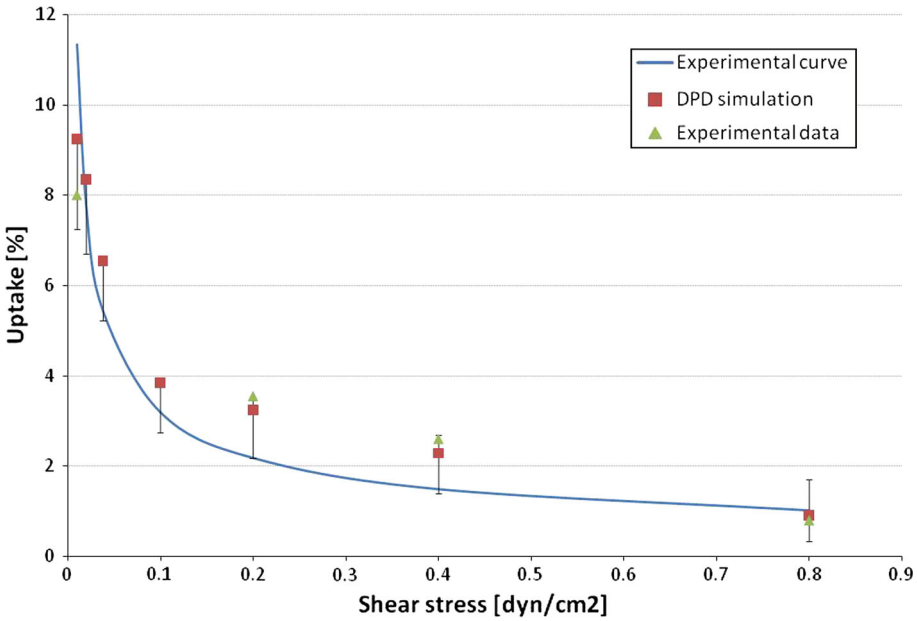

Fig. 7 Results obtained from experimental measurement and DPD simulations. Experimental curve (*blue line*) is fitted with data obtained from experiment (*green triangles*). *Red rectangles* represent average values obtained from several DPD simulations for certain shear stress. Standard deviation from experimental results is 1.1550448. It can be observed that DPD calculation give similar results with experimental data, after averaging results from certain number of calculations due to stochastic nature of technique (color figure online)

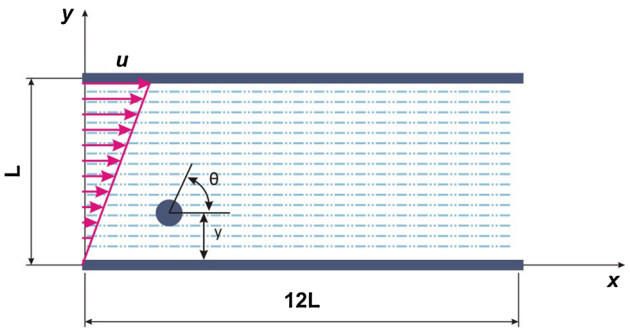

Fig. 8 Geometrical data necessary for the simulation

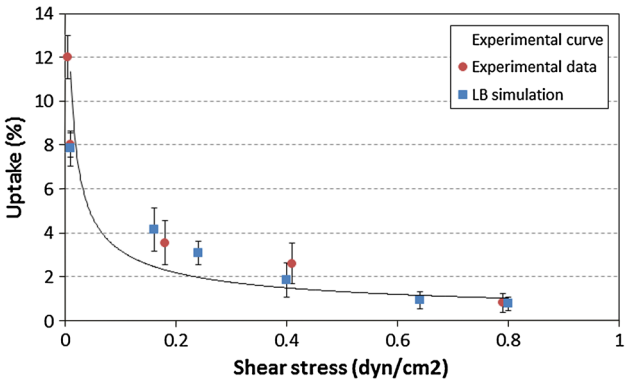

Fig. 9 Variation in LDL uptake for different values of shear stress. Experimental curve is fitted with data obtained from experiment (and given on *diagram* with *red dots*). *Blue squares* represent the results obtained from particle tracking simulation (standard deviation from experimental data is 0.98) (color figure online)

conditions are set such that velocity of the bottom wall is equal to zero and velocity of the upper wall is set to the maximum value. The maximum value varies, in order to obtain different shear stress rates and to obtain the desired diagram of variation of LDL uptake with different shear stress values. As initial condition, the shear flow velocity is imposed on both left and right wall of the domain. The length and the height of the domain are obtained from the experimental setup data. Using these physical dimensions of the domain, the number of lattice nodes for both axes is calculated. Overall 17,500 nodes in the lattice mesh is used for LB simulations. Particle tracking approach was used to estimate the percentage of LDL uptake for different shear stress rates.

The number of LDL particles in the initial configuration is taken to be 1.3 ‰ of the overall number of particles. In this case, with overall 17,500 particles in the lattice mesh, the number of LDL particles is taken to be 23. Overall 8 simulations with random distribution of LDL particles were performed, and the average value of uptake is evaluated. The obtained results for LB simulation are shown in Fig. 9.

4 Discussion and conclusion

High accumulation of macromolecules, i.e., LDL molecules, within the arterial wall is a very important factor in atherosclerosis (Stangeby and Ethier 2002b; Soulis et al. 2008). It was concluded that atherosclerosis is observed in those regions of the artery with local abnormalities of wall shear stress (Soulis et al. 2006) and locally high concentrations of LDL molecules (Deng et al. 1995). The transport of LDL molecules through blood flow in cardiovascular

system has large influence in the genesis and progression of atherosclerosis (Fatouraee et al. 1998), and therefore, the modeling of transport of LDL molecules became the topic of many research papers. Among several LDL transport models, there are three major categories. The simplest models are wall-free models, in which the arterial wall is substituted by a simplified boundary condition and the macromolecular transport in the arterial wall is analyzed (Rappitsch and Perktold 1996; Wada and Karino 2000). In lumen-wall models, the transport within the lumen and the wall is coupled (Moore and Ethier 1997; Stangeby and Ethier 2002a, b). Also, there are multilayer models, which break the arterial wall down into several layers and model the transport of molecules through the arterial wall and lumen (Yuan et al. 1991; Huang et al. 1994; Huang and Tarbell 1997; Tada and Tarbell 2004; Fry 1985, 1987; Karner et al. 2001).

In this study, in both experiment and numerical simulation, we observed that with lower wall shear stress rates, the number of bound LDL molecules increases. This is in accordance with the findings previously published in the literature. Deng et al. (1995) performed both computational and experimental studies of canine carotid arteries, and they came to the conclusion that lipids accumulate at endothelial surfaces where blood velocity and shear stress are low. But, they only tested this effect indirectly and did not measure directly the concentration of macromolecules under different wall shear rates and filtration velocities, like it was done in this study. Sun et al. (2006) investigated the influence of wall shear stress on transport of molecules through blood and concluded that high concentration of LDL molecules appears in low shear stress regions. Also, Olgac et al. (2008) modeled LDL transport using a coupled blood-wall mass transport model. They calculated parameters of the model in terms of the local wall shear stress and observed high LDL concentrations in the arterial wall in low shear stress regions.

However, most of these numerical models use continuum-based methods, such as the finite element method to simulate the transport of molecules (Yang and Vafai 2006; Sun et al. 2006). In the present study, the LDL molecules were considered as solid bodies within plasma. This assumption enabled us to perform computational analysis of binding of LDL molecules to the arterial wall using discrete methods and considering the dynamics of discrete particles.

The coupling of experimental data with numerical simulations is mostly performed in terms of measurements of appropriate model parameters (Yang and Vafai 2006; Sun et al. 2006), while in this study, we compared computational results obtained from DPD and LB simulations with experimental results for LDL transport through isolated blood vessel. Additional binding forces are calculated using computational chemistry, where the energy of binding of LOX-1 receptor with glutamine acid is calculated.

From the presented study, it is evident that DPD and LB methods can be applied for modeling atherosclerosis problems and for investigating binding of LDL molecules to endothelium of blood vessel. Good agreement of experimental and numerical results shows a potential benefit for prediction of development and progression of atherosclerosis using computer modeling. Future work will focus on extending the present model to a more complex model. Coupling the computational chemistry with these two discrete modeling approaches will enable us to obtain more accurate results and further investigate the complex process of atherosclerosis.

Acknowledgments The part of this research is supported by Ministry of Education and Science in Serbia, Grants III41007, ON174028, and FP7 ICT-2007-2-5.3 (224297) ARTreat Project.

References

Bhatnagar PL, Gross EP, Krook M (1954) A model for collision processes in gases. I. Small amplitude processes in charged and neutral one-component systems. Phys Rev E 77:511–525

Bickel PE, Freeman M (1992) Rabbit aortic smooth muscle cells express inducible macrophage scavenger receptor messenger RNA that is absent from endothelial cells. J Clin Invest 90:1450–1457

Chen M, Kakutani M, Minami M (2000) Increased expression of lectin-like oxidized low density lipoprotein receptor-1 in initial atherosclerotic lesions of Watanabe heritable hyperlipidemic rabbits. Arterioscl Thromb Vasc Biol 20:1107–1115

Deng X, Marois Y, Merhi Y, How T, King M, Guidoin R et al (1995) Luminal surface concentration of lipoprotein (LDL) and its effect on the wall uptake of cholesterol by canine carotid arteries. J Vasc Surg 21(1):135–145

Đukić T (2012) Modelling solid-fluid interaction using LB method. Master Thesis, University of Kragujevac

Espanol P, Warren P (1995) Statistical mechanics of dissipative particle dynamics. Europhys Lett 30:191–196

Fatouraee N, Deng X, De Champlain A, Guidoin R (1998) Concentration polarization of low density lipoproteins (LDL) in the arterial system. Ann NY Acad Sci 11(5):137–146

Filipovic N, Kojic M, Tsuda A (2008a) Modeling thrombosis using dissipative particle dynamics method. Phil Trans R A 366(1879): 3265–3279

Filipovic N, Ravnic DJ, Kojic M, Mentzer SJ, Haber S, Tsuda A (2008b) Interactions of blood cell constituents: experimental investigation and computational modeling by discrete particle dynamics algorithm. Microvasc Res 75:279–284

Fry DL (1985) Mathematical models of arterial transmural transport. Am J Physiol 248:H240–H263

Fry DL (1987) Mass transport, atherogenesis and risk. Arteriosclerosis 7:88–100

Groot RD, Warren PB (1997) Dissipative particle dynamics: bridging the gap between atomistic and mesoscopic simulation. J Chem Phys 107:4423–4435

Hansson GK (2005) Inflammation, atherosclerosis, and coronary artery disease. N Engl J Med 352:1685–1695

Hoogerburgge PJ, Koelman JM (1992) Simulating microscopic hydrodynamic phenomena with dissipative particle dynamics. Europhys Lett 19:155–160

Huang ZJ, Tarbell JM (1997) Numerical simulation of mass transfer in porous media of blood vessel walls. Am J Physiol 273:H464–H477

Huang Y, Rumschitzki D, Chien S, Weinbaum S (1994) A fiber matrix model for the growth of macromolecular leakage spots in the arterial intima. J Biomech Eng 116:430–445

Karner G, Perktold K, Zehentner HP (2001) Computational modeling of macromolecule transport in the arterial wall. Comput Meth Biomech Biomed Eng 4:491–504

Kataoka H, Miyamoto S (1999) Expression of lectin-like oxidized low-density lipoprotein receptor-1 in human atherosclerotic lesions. Circulation 99:3110–3117

Kriško A, Etchebest C (2006) Theoretical model of human apolipoprotein B100 tertiary structure. Proteins 66:342–358

Kume N, Sawamura T, Moriwaki H, Aoyama A, Nishi E, Ueno Y et al (1998) Inducible expression of LOX-1, a novel lectin-like receptor for oxidized low density lipoprotein, in vascular endothelial cells. Circ Res 83:322–327

Li D, Mehta JL (2000a) Upregulation of endothelial receptor for oxidized LDL (LOX-1) by oxidized LDL and implications in apoptosis of human coronary artery endothelial cells: evidence from use of antisense LOX-1 mRNA and chemical inhibitors. Arterioscl Thromb Vasc Biol 20:1116–1122

Li D, Mehta JL (2000b) Antisense to LOX-1 inhibits oxidized LDL-mediated upregulation of monocyte chemoattractant protein-1 and monocyte adhesion to human coronary artery endothelial cells. Circulation 101:2889–2895

Libby P (2002) Inflammation in atherosclerosis. Nature 420:868–874. Molecular Operating Environment version 2009.10, Chemical Computing Group Inc. Montreal, Canada

Lin SJ, Jan KM, Schuessler G, Weinbaum S, Chien S (1988) Enhanced macromolecular permeability of aortic endothelial cells in association with mitosis. Atherosclerosis 73:223–232

Lusis AJ (2000) Atherosclerosis. Nature 407:233–241

Malaspinas OP (2009) Lattice Boltzmann method for the simulation of viscoelastic fluid flows. PhD dissertation, University of Switzerland

Moore JA, Ethier CR (1997) Oxygen mass transfer calculations in large arteries. J Biomech Eng 119:469–475

MOPAC (2009) Available on-line from http://openmopac.net/MOPAC2009.html

Murase T, Kume N, Korenaga R, Ando J, Sawamura T, Masaki T et al (1998) Fluid shear stress transcriptionally induces lectin-like oxidized LDL receptor-1 in vascular endothelial cells. Circ Res 83:328–333

Nagase M, Hirose S, Sawamura T, Masaki T, Fujita T (1997) Enhanced expression of endothelial oxidized low-density lipoprotein receptor (LOX-1) in hypertensive rats. Biochem Biophys Res Co 237:496–498

Ohki I, Ishigaki T, Oyama T, Matsunaga S, Xie Q, Ohnishi-Kameyama M, Murata T, Tsuchiya D, Machida S, Morikawa K, Tate S (2005) Crystal structure of human lectin-like, oxidized low-density lipoprotein receptor 1 ligand binding domain and its ligand recognition mode to OxLDL. Structure 13:905–917

Olgac U, Kurtcuoglu V, Poulikakos D (2008) Computational modeling of coupled blood–wall mass transport of LDL: effects of local wall shear stress. Am J Physiol Heart Circ Physiol 294(2):909–919

Rappitsch G, Perktold K (1996) Pulsatile albumin transport in large arteries: a numerical simulation study. J Biomech Eng 118: 511–519

Reiss AB, Anwar K, Wirkowski P (2009) Lectin-like oxidized low density lipoprotein receptor 1 (LOX-1) in atherogenesis: a brief review. Curr Medic Chem 16:2641–2652

Sawamura T, Kume N, Aoyama T, Moriwaki H, Miwa S, Kita T, Masaki T (1997) An endothelial receptor for oxidized low-density lipoprotein. Nature 386:73–77

Soulis JV, Farmakis TM, Giannoglou GD, Louridas GE (2006) Wall shear stress in normal left coronary artery tree. J Biomech 39(4):742–749

Soulis JV, Giannoglou GD, Papaioannou V, Parcharidis GE, Louridas GE (2008) Low density lipoprotein concentration in the normal left coronary artery tree. Biomed Eng Online 17:7–26

Stangeby DK, Ethier CR (2002a) Coupled computational analysis of arterial LDL transport—effects of hypertension. Comput Meth Biomech Biomed Eng 5:233–241

Stangeby DK, Ethier CR (2002b) Computational analysis of coupled blood-wall arterial LDL transport. J Biomech Eng 124:1–8

Stewart JJP (2007) Optimization of parameters for semiempirical methods V: modification of NDDO approximations and application to 70 elements. J Mol Model 13:1173–1213

Sun N, Wood NB, Hughes AD, Thom SAM, Xu XY (2006) Fluid-wall modelling of mass transfer in an axisymmetric stenosis: effects of shear-dependent transport properties. Ann Biomed Eng 34:1119–1128

Tada S, Tarbell JM (2004) Internal elastic lamina affects the distribution of macromolecules in the arterial wall: a computational study. Am J Physiol 287:H905–H913

Wada S, Karino T (2000) Computational study on LDL transfer from flowing blood to arterial walls. In: Yamaguchi T (ed) Clinical applications of computational mechanics to the cardiovascular system. Springer, Berlin, pp 157–173

Wolfram S (1986) Cellular automaton fluids 1: basic theory. J Stat Phys 45:471–526

Yang N, Vafai K (2006) Modeling of low-density lipoprotein (LDL) transport in the artery—effects of hypertension. Int J Heat Mass Transfer 49(5):850–867

Yuan F, Chien S, Weinbaum S (1991) A new view of convective–diffusive transport processes in the arterial intima. J Biomech Eng 133:314–329